THE JOURNAL OF PHYSICAL CHEMISTRY A

Article

pubs.acs.org/JPCA

# Role of Aggregates in the Luminescence Decay Dynamics of Conjugated Polymers

Rajarshi Chakraborty[†] and Lewis J Rothberg[*,‡]

[†]Materials Science Program, University of Rochester, Rochester, New York 14627, United States

[‡]Department of Chemistry, University of Rochester, Rochester, New York 14627, United States

**ABSTRACT:** Fluorescence quantum yields of conjugated polymer films are systematically lower than their counterparts in dilute solution. Films also exhibit a long "temporal tail" in their fluorescence decay dynamics not present in solution. We study the spectroscopy, excitation wavelength dependence, temperature dependence, and electric field quenching of the temporal tail of the photoluminescence in MEH-PPV on a nanosecond time scale to elucidate the relationship between those observations. We conclude that the tail represents emission from H-like aggregated regions in the polymer. Using a simple model of the photophysics, we estimate the formation yield of the aggregates responsible for the tail emission to be <20% so that they cannot account for the large reduction in fluorescence observed in densely packed films relative to that in solution.

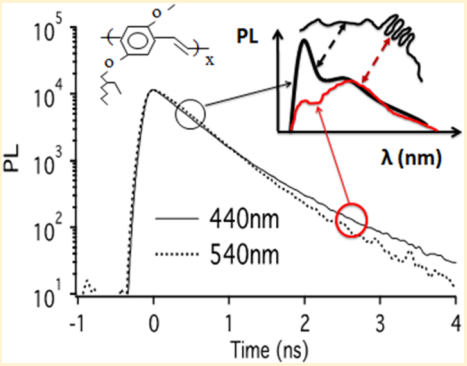


## I. INTRODUCTION

Luminescent conjugated polymers are potentially useful for applications in display technology,[1−3] solid-state lighting,[4,5] and biomolecular sensing.[6−9] One important materials challenge relevant to these applications is to understand and mitigate aggregation quenching, the reduction of luminescence when conjugated chromophores interact.[10−15] Typically, aggregation is correlated with red-shifted spectra and a long temporal tail to the photoluminescence (PL) decay dynamics.[13] Our purpose here is to understand the origin of that tail and determine whether it is associated with the mechanism of aggregation quenching. We therefore study the spectrum of the temporal tail of MEH-PPV PL and how it depends on excitation wavelength and applied electric field. What we find is that the spectral dynamics in MEH-PPV are consistent with a relatively long-lived population of weakly emissive sites that we associate with aggregates. The formation yield of the aggregates increases with decreasing excitation wavelength, but, unfortunately, the formation yield of long-lived aggregates cannot explain the large decrease in PL observed with increased packing order. The dependence of the excitonic and aggregate emission with applied field indicates that the aggregated species responsible for long-lived emission are formed preferentially in regions susceptible to field quenching. We try to place these results in the context of other work on MEH-PPV photophysics, particularly as it pertains to the root cause of aggregation quenching.

## II. EXPERIMENTAL SECTION

**Sample Preparation.** MEH-PPV (poly[2-methoxy-5-(2-ethylhexyloxy)-1,4-phenylenevinylene]) was obtained from Sigma-Aldrich in powder form having average molecular weight of $10^6$ g/mol. Ten mg of MEH-PPV was dissolved in 10 mL of chloroform and stirred overnight. Several drops of the solution were added to chloroform in a 1 cm path length clean quartz cuvette for absorption and photoluminescence measurements. Spin-cast films were made by placing few drops of the stock solution onto clean 2 mm thick quartz discs of radius 2 cm, followed by spinning at 1200 rpm for 1 min. Drop-cast films were made by casting several drops of stock solution onto the clean quartz discs, and the samples were left to dry for at least 10 min in the dark prior to use.

**Steady-State Spectroscopy.** Absorption measurements were carried out at room temperature using a Cary 60 UV−vis spectrophotometer. Photoluminescence spectra were collected using an Ocean Optics S2000 spectrometer with 100 ms integration time and three data averages. The excitation source was a Fianium SC 480-20 broadband fiber laser. The sample was excited and photoluminescence was collected from the free (nonsubstrate) face of the film in all cases, including the transient measurements described later. The excitation wavelength was selected using either a linear bandpass filter or the Fianium Acousto-Optic Tunable Filter (AOTF), each providing ∼10 nm excitation bandwidth. Steady-state emission spectra were also collected using a Horiba Yvon Fluoromax 3 fluorometer for quantitative calibration of the relative intensities at different emission wavelengths.

For relative fluorescence yield measurements versus excitation wavelength, we used the SC 480-20 and drop-cast samples as above but detected undispersed fluorescence with a photomultiplier as the Fianium excitation wavelength was tuned. The excitation power at each wavelength was obtained

Received: November 19, 2015
Revised: January 8, 2016
Published: January 8, 2016





DOI: 10.1021/acs.jpca.5b11349
J. Phys. Chem. A 2016, 120, 551−555

using an Ophir Nova 7Z01500 power meter. Relative quantum yield was obtained by dividing the emission intensity by the excitation power. A correction for sample absorbance was also made but was negligible except at the extreme red edge of the absorption because the drop-cast samples under study were optically thick.

**Field-Quenching Measurements.** Devices were fabricated using indium tin oxide (ITO)-coated glass substrates obtained from Tinwell Technology and thoroughly cleaned by washing with Alconox Detergent. The cleaned substrates were sonicated for ∼10 min in deionized water, followed by sonication in isopropanol and then acetone for 10 min each. The wet samples were blown dry with flowing nitrogen gas and MEH-PPV films were drop cast and dried as above. Vacuum evaporation of an aluminum contact at base pressures of $\sim 10^{-6}$ Torr completed the device architecture (ITO (80 nm)/MEH-PPV (∼1 micron)/Al (100 nm)).

**Transient Photoluminescence.** The fluorescence decay curves were recorded using time-correlated single-photon counting (TCSPC)[16] using the wavelength-selected Fianium SC 480-20 with 20 MHz repetition rate as excitation source (typical pump powers of a few microwatts with spot size ∼2 mm). Photons collected by an avalanche photodiode (APD) were referenced in time to the electrical signal produced by a fast photodiode monitoring the intracavity pulse train. This procedure results in high photon counting rates ($\sim 5 \times 10^5$ Hz) but relatively poor time resolution (∼150 ps). Scattered light was used to generate an instrument response function used for deconvolution. To extract transient spectra, we recorded PL decay curves at many wavelengths defined by bandpass filters placed in front of the APD. The amplitudes of the various decay curves were adjusted by forcing their integrated intensities to conform to the relative intensities of the corresponding wavelengths in the calibrated PL spectra produced by the fluorometer. Thus, transient emission spectra $S(\lambda, t_1 \rightarrow t_2)$ are determined for an interval from $t_1$ to $t_2$ using eq 1.

$$S(\lambda_j, t_1 \rightarrow t_2) = \frac{\left(\int_{t_1}^{t_2} G(\lambda_j, t)\, dt\right) \times F(\lambda_j)}{\left(\int_0^{\infty} G(\lambda_j, t)\, dt\right)} \quad (1)$$

where $F(\lambda_j)$ is the intensity of steady-state PL at wavelength $\lambda_j$ and $G(\lambda_j, t)$ is the PL decay curve at wavelength $\lambda_j$. For 300 K measurements, the films were placed in a transparent cell under nitrogen flow. For 77 K measurements, the films were placed in a finger dewar and immersed in liquid nitrogen.

## III. RESULTS AND DISCUSSION

**Identification of the Tail Species as Aggregates.** Figure 1 presents PL spectra from MEH-PPV with various degrees of ordering/aggregation, comparing samples in chloroform solution to spin-cast and drop-cast films. These spectra have minor dependence on excitation wavelength compared with the large changes that take place due to changes in processing and environment. We ascribe the red shift in the PL spectra with increasing aggregation to packing-induced planarization resulting in longer conjugation lengths because similar shifts are observed that occur in both absorption and emission. While it is difficult to compare PL intensities from sample to sample quantitatively, it is clear that the drop-cast film emission is weaker than that of even much thinner spin-cast films. Companion PL decay dynamics are shown in Figure 2, where we have excited the samples using wavelengths having nearly

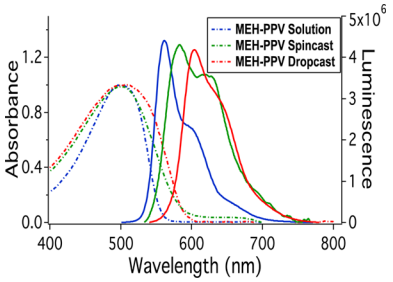


**Figure 1.** Absorption and PL spectra of MEH-PPV chloroform solution, spin-cast and drop cast films recorded at 300 K. The PL is excited at 480 nm.

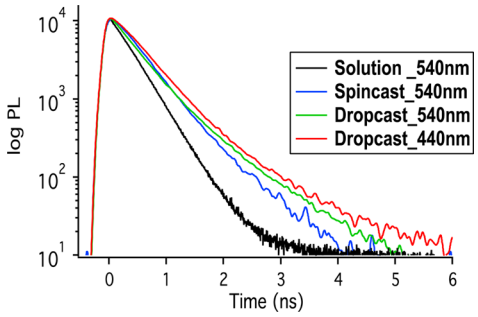


**Figure 2.** PL decay dynamics corresponding to the solutions and films in Figure 1. Excitation wavelengths are as noted in the legend.

equal absorbance (440 and 540 nm) to minimize artifacts due to differences in morphology or degree of oxidation with distance from the surface of the film. These data are typical of what is observed upon aggregation and ordering of conjugated polymers. A red shift is observed, and a long temporal tail to the PL emerges. Despite the fact that the average decay time for the PL is not very different, the quantum yield in more aggregated samples is greatly diminished,[13] an observation difficult to reconcile with conventional photophysical models.

The pulse energies used in our experiments are much lower than those where exciton−exciton interactions are observed.[17] The dynamics observed in Figure 2 do not vary with excitation pulse energy, and the luminescence intensity is strictly linear with photoexcitation fluence. These observations rule out triplet−triplet annihilation as the underlying reason for the long-lived PL. The data also show that bluer excitation leads to a greater proportion of the PL coming from the temporal tail. Insight into the origin of the tail is provided by an analysis of the tail spectrum, derived from measurements of the PL decay dynamics at many different wavelengths while correcting the integrated intensities to agree with the steady-state PL spectrum (see above). To have the best signal-to-noise ratios, we confine ourselves to drop-cast samples where the tail is much larger. At both 77 and 300 K, the long-lived luminescence is red-shifted and appears nearly unstructured, as shown in Figure 3. While these features are characteristic of excimer emission, several observations tend to rule out a description of the emitters as excimers. First, a substantial portion of the emission is just as blue as the prompt excitonic ($S_1$) fluorescence. In addition, the spectrum is much bluer and shorter lived than the spectrum assigned to excimer emission in previous literature.[12] For this reason, we think that the best description of this emission would be as coming from something more like aggregated regions organized to give them predominant H-like character.[14,15] As shown by


DOI: 10.1021/acs.jpca.5b11349
J. Phys. Chem. A 2016, 120, 551−555

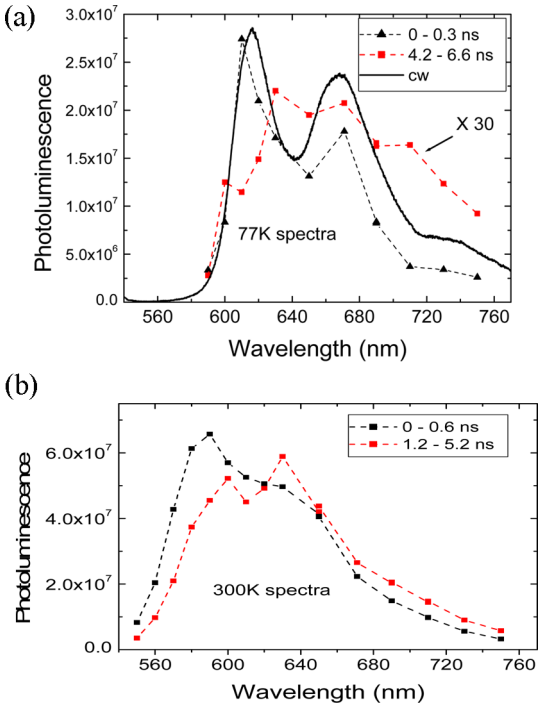


**Figure 3.** (a) Transient emission spectra at short and long times after photoexcitation with 520 nm pulses at (a) 77 and (b) 300 K. These are inferred from wavelength-dependent dynamics as described in the text. The time windows for spectral integration are selected to be good representations of the prompt and long-lived photoluminescence while maintaining good signal-to-noise ratios.

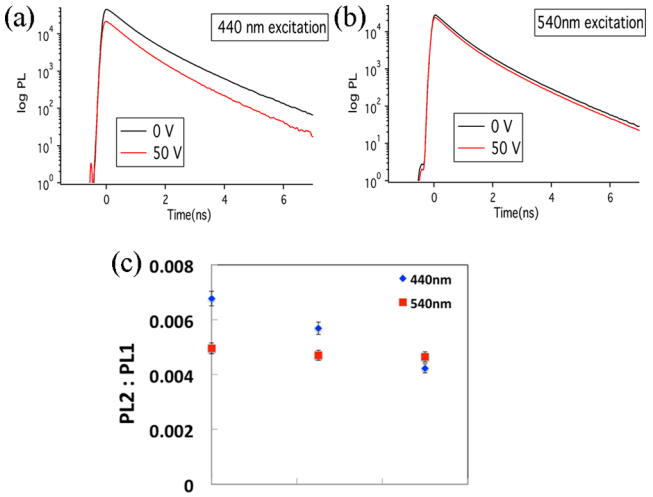


**Figure 4.** (a) Decay dynamics of integrated photoluminescence following photoexcitation of MEH-PPV at (a) 440 nm or (b) 540 nm in a reverse biased device structure with and without an applied voltage. (c) Ratio of delayed to prompt photoluminescence (PL2/PL1) versus excitation wavelength and applied field.

Spano,[18,19] these would have formally forbidden 0−0 bands, giving them longer lifetime and apparently red-shifted spectra. The lack of vibronic structure and emission extending just as blue as the exciton suggests that we are observing a very inhomogeneous distribution of emissive sites spanning the spectrum from aggregated sites with moderate to very small J-like character. The delayed emission we observe at 77 K does not resemble the ordered red-phase spectrum deduced in the beautiful work of Köhler and coworkers,[19,20] and those differences can be ascribed to the fact that the MEH-PPV chains are prevented from aggregating by their MeTHF host matrix in those studies.

**Formation Mechanism of the Excited States at Aggregated Sites.** Previous work has found that delayed photoluminescence in MEH-PPV on the microsecond time scale comes primarily from geminate recombination of photogenerated charge (polaron) pairs.[21,22] We set out to ascertain whether the tail emission we observe on the nanosecond time scale could be derived from that pathway. We reasoned that if this was the case then the behavior of the temporal tail would be altered dramatically by a substantial electric field applied to MEH-PPV films made inside a reverse-biased ITO/MEH-PPV/Al diode (Figure 4). In previous experiments by Khan et al.,[23] this resulted in both reduction of the initial PL intensity ("amplitude quenching") and reduction of the excited-state lifetime ("lifetime quenching"). Unfortunately, these authors did not study the spectroscopy of the temporal tail or remark on its behavior with applied field. Probably because we used nearly an order of magnitude smaller field, we observed only amplitude quenching that is presumably due to the ability of the field to ionize excitons into charge pairs during the first few picoseconds after the excitons are formed while they remain "hot". Consistent with that interpretation, the amplitude quenching is substantially larger for blue (440 nm) than for red (540 nm) excitation (Figure 4b); however, the amount of suppression of the temporal tail by the field is nearly identical to the amount of suppression of the excitons for 540 nm excitation. As can been seen in Figure 4, the overall intensity is reduced by the application of the field, but the dynamics are not dramatically different. The clear implication is that tail is not due to charge pair recombination and it is reasonable to conclude that the aggregated sites must be populated via energy transfer from excitons that happens on a longer time scale than the field dissociation associated with amplitude quenching.

With 440 nm excitation, however, we observe that the tail emission is quenched substantially more than the short-lived excitonic emission (Figure 4c. Our interpretation of that observation supports the general idea behind the tail representing emission from regions with much more H-like character. The J-like regions in MEH-PPV represent primarily intrachain coupling[18] that occurs in disordered regions, while the H-like regions derive from the ordered, packed regions. In keeping with the general principles governing J and H aggregation where the lowest transition of H aggregates carries little oscillator strength,[24] we suppose that regions excited in the lowest energy state (i.e., at 540 nm) are more J-like and regions excited at higher photon energies (i.e., 440 nm) have more H-character.[18] This is consistent with the substantially increased amount of tail emission (Figure 2) when exciting at bluer wavelengths that presumably represents preferential excitation of H-like aggregated regions. We also expect the field to be much more effective at quenching excited states when we excite into packed regions with strong interchain coupling, consistent with the much larger amplitude quenching by the applied field observed for 440 nm excitation (Figure 4). At 540 nm, nearly all of the temporal tail emission comes from excitation of isolated regions, followed by migration to more ordered regions, so that the main emission (PL1) and the temporal tail emission (PL2) are quenched to a similar degree (Figure 4c). At 440 nm, however, some fraction of the excitation is directly into the second band for the H-like


DOI: 10.1021/acs.jpca.5b11349
J. Phys. Chem. A 2016, 120, 551−555

regions, where field quenching of excitations is much stronger and the effect on the temporal tail is therefore greatly enhanced relative to quenching following excitation of unpacked regions.

**Quantification of Aggregate Site Formation Efficiency.** A central question we want to address here is whether the emissive sites associated with the PL tail are formed with high enough probability to be responsible for the diminution in fluorescence quantum yield associated with aggregation. We can use the dependence of luminescence efficiency on excitation wavelength (Figure 5) to estimate the aggregate

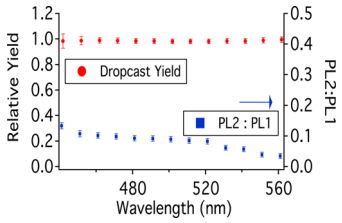


**Figure 5.** Relative quantum yield and ratio of prompt versus delayed PL versus excitation wavelength for a thick drop-cast sample of MEH-PPV.

quantum yield and its wavelength dependence as follows. Assuming a kinetic scheme like that in Figure 6, we can write an

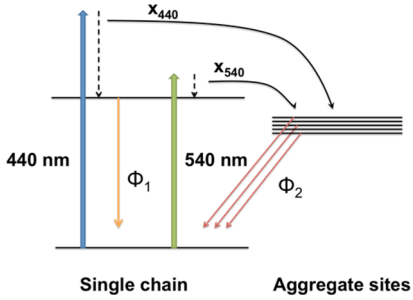


**Figure 6.** Photophysical scheme used for modeling our data to estimate formation quantum yields of aggregates responsible for the emissive tail.

expression for the ratio $R_\lambda$ of PL from the aggregate ($PL_2$) to PL from the exciton ($PL_1$)

$$R_\lambda = (PL_2/PL_1)_\lambda = x_\lambda\Phi_2/(1 - x_\lambda)\Phi_1 = x_\lambda\eta/(1 - x_\lambda) \quad (2)$$

where $\Phi_2$ and $\Phi_1$ are the emissive efficiency of the aggregate and exciton, respectively, and we have defined their ratio as $\eta$. The quantities $x_\lambda$ refer to the fractions of excitations that form aggregates after excitation at wavelength $\lambda$. We can estimate the ratio of aggregate to exciton PL ($PL_2/PL_1$) from our dynamics data (Figure 2) excited at $\lambda$ = 440 nm ($R_{440}$) and $\lambda$ = 540 nm ($R_{540}$). This is done by fitting the data to a biexponential after deconvolution of the instrument response and using the integrated intensities of the two exponential components. We can also estimate the relative amounts of total PL emitted when exciting with equal numbers of absorbed photons at these two wavelengths, $C$, from steady-state integrated PL data, where we can write $C$ as

$$C = (PL_1 + PL_2)_{440}/(PL_1 + PL_2)_{540} \quad (3)$$

where, of course,

$$(PL_1 + PL_2)_\lambda = (1 - x_\lambda)\Phi_1 + x_\lambda\Phi_2 \quad (4)$$

This analysis enables us to use three measurements ($R_{440}$, $R_{540}$, and $C$) to specify the three unknowns $x_{440}$, $x_{540}$ (fractions of aggregates formed after 440 and 540 nm excitation), and $\eta$ (relative emissive efficiency of aggregates and excitons). Equations 2−4 can be solved to produce the following expressions

$$\eta = [CR_{440}(1 + R_{540}) - R_{540}(1 + R_{440})]/ /[1 + R_{440} - C - CR_{540}] \quad (5)$$

$$x_{440} = R_{440}/(\eta + R_{440}); \quad x_{540} = R_{540}/(\eta + R_{540}) \quad (6)$$

Using $R_{440}$ = 0.014, $R_{540}$ = 0.010, and $C$ = 0.98 ± 0.05, we obtain aggregate yields of $x_{440}$ = 0.05 + 0.25/−0.05 and $x_{540}$ = 0.04 + 0.18/−0.04. While these are quite large ranges, the relatively small and nearly excitation wavelength-independent yields of aggregates are consistent with previous studies that indicate that the major reason for reduced quantum yield in aggregated MEH-PPV has to do with processes on a several picosecond time scale that repopulate the ground state.[25] Apparently, there is additional diminution of yield due to aggregate formation, although we point out that we purposely induced strong interchain processes by using drop casting with slow solvent evaporation to make samples with especially large temporal tails in their excited-state PL. From the same data and eq 5, we obtain a relative emissive efficiency of the aggregate $\eta$ ≈1.7% at ambient temperatures, which seems reasonable.

## IV. CONCLUSIONS

We have studied the behavior of the long temporal tail in the PL decay dynamics of MEH-PPV, typical of that from conjugated polymers in aggregated states. Measurements of the spectral dynamics, excitation wavelength dependence, field quenching, and temperature dependence of the photoluminescence are consistent with a picture where the long-lived emission is from H-like aggregates predicted by Spano in regions with strong interchain coupling. Using a simple model, we are able to estimate the fraction of photoexcitations that lead to aggregate emission to be at most 20%, a value too small to explain the reduction of fluorescence quantum yield observed with aggregation. Our conclusion further underscores the need to understand fast internal conversion processes that are apparently enhanced by aggregation and can lead to low luminescence yield in conjugated polymer films.[25]

## AUTHOR INFORMATION

### Corresponding Author

*E-mail: rothberg@chem.rochester.edu.

### Notes

The authors declare no competing financial interest.

## ACKNOWLEDGMENTS

We thank Al Marchetti and Ralph Young for helpful discussions. We also thank Lisong Xu for fabricating the device structures used for field quenching studies. We gratefully acknowledge support under NSF DMR-1105355.

## REFERENCES

(1) Friend, R. H.; Gymer, R. W.; Holmes, A. B.; Burroughes, J. H.; Marks, R. N.; Taliani, C.; Bradley, D. D. C.; Dos Santos, D. A.; Brédas, J. L.; Löglund, M.; Salaneck, W. R. Electroluminescence in Conjugated Polymers. *Nature* **1999**, *397*, 121−128.



DOI: 10.1021/acs.jpca.5b11349
J. Phys. Chem. A 2016, 120, 551−555

(2) Yim, K. H.; Whiting, G. L.; Murphy, C. E.; Halls, J. J. M.; Burroughes, J. H.; Friend, R. H.; Kim, J.-S. Controlling Electrical Properties of Conjugated Polymers Via a Solution-Based p-type Doping. *Adv. Mater.* **2008**, *20*, 3319−3324.
(3) Borchardt, J. K. Developments in Organic Displays. *Mater. Today* **2004**, *7*, 42−46.
(4) AlSalhi, M. S.; Alam, J.; Dass, L. A.; Raja, M. Recent Advances in Conjugated Polymers for Light Emitting Devices. *Int. J. Mol. Sci.* **2011**, *12*, 2036−2054.
(5) Ying, L.; Ho, C. L.; Wu, H.; Cao, Y.; Wong, W.-Y. White Polymer Light-Emitting Devices for Solid-State Lighting: Materials, Devices and Recent Progress. *Adv. Mater.* **2014**, *26*, 2459−2473.
(6) Liu, B.; Bazan, G. C. Homogeneous Fluorescence Bbased DNA Detection with Water Soluble Conjugated Polymers. *Chem. Mater.* **2004**, *16*, 4467−4476.
(7) Pinto, M. R.; Schanze, K. S. Amplified Fluorescence Sensing of Protease Activity with Conjugated Polyelectrolytes. *Proc. Natl. Acad. Sci. U. S. A.* **2004**, *101*, 7505−7510.
(8) Pu, K. Y.; Liu, L. B. Conjugated Polyelectrolytes as Light-Up Macromolecular Probes for Heparin Sensing. *Adv. Funct. Mater.* **2009**, *19*, 277−284.
(9) Rochat, S.; Swager, T. M. Fluorescence Sensing of Amine Vapors Using a Cationic Conjugated Polymer Combined with Various Anions. *Angew. Chem., Int. Ed.* **2014**, *53*, 9792−9796.
(10) Yan, M.; Rothberg, L. J.; Kwock, E. W.; Miller, T. M. Interchain Excitations in Conjugated Polymers. *Phys. Rev. Lett.* **1995**, *75*, 1992−1995.
(11) Nguyen, T. Q.; Martini, I. B.; Liu, J.; Schwartz, B. J. Controlling Interchain Interactions in Conjugated Polymers: The Effects of Chain Morphology on Exciton-Exciton Annihilation and Aggregation in MEH-PPV Films. *J. Phys. Chem. B* **2000**, *104*, 237−255.
(12) Jakubiak, R.; Collison, C. J.; Wan, W. C.; Rothberg, L. J.; Hsieh, B. R. Aggregation Quenching of Luminescence in Electroluminescent Conjugated Polymers. *J. Phys. Chem. A* **1999**, *103*, 2394−2398.
(13) Collison, C. J.; Rothberg, L. J.; Treemaneekarn, V.; Li, Y. Conformational Effects on the Photophysics of Conjugated Polymers: A Two Species Model for MEH-PPV Spectroscopy and Dynamics. *Macromolecules* **2001**, *34*, 2346−2352.
(14) Spano, F. C. Excitons in Conjugated Oligomer Aggregates, Films, and Crystals. *Annu. Rev. Phys. Chem.* **2006**, *57*, 217−243.
(15) Egelhaaf, H. J.; Gierschner, J.; Oelkrug, D. Characterization of Oriented Oligo(phenylenevinylene) Films and Nano-Aggregates by UV/Vis-Absorption and Fluorescence Spectroscopy. *Synth. Met.* **1996**, *83*, 221−226.
(16) Phillips, D.; O'Connor, D. V. *Time-Correlated Single Photon Counting*; Academic Press, 1984.
(17) Kepler, R. G.; Valencia, V. S.; Jacobs, S. J.; McNamara, J. J. Exciton-Exciton Annihilation in Poly(p-phenylenevinylene). *Synth. Met.* **1996**, *78*, 227−230.
(18) Spano, F. C.; Silva, C. H- and J-Aggregate Behavior in Polymeric Semiconductors. *Annu. Rev. Phys. Chem.* **2014**, *65*, 477−500.
(19) Yamagata, H.; Hestand, N. J.; Spano, F. C.; Köhler, A.; Scharsich, C.; Hoffmann, S. T.; Bässler, H. The Red-Phase of Poly[2-methoxy-5-(2-ethylehexoxy)-1,4-phenylenevinylene] (MEH-PPV): A Disordered HJ-Aggregate. *J. Chem. Phys.* **2013**, *139*, 114903.
(20) Köhler, A.; Hoffmann, S. T.; Bässler, H. An Order-Disorder Transition in the Conjugated Polymer MEH-PPV. *J. Am. Chem. Soc.* **2012**, *134*, 11594−11601.
(21) Schweitzer, B.; Arkhipov, V. I.; Scherf, U.; Bassler, H. Geminate Pair Recombination in a Conjugated Polymer. *Chem. Phys. Lett.* **1999**, *313*, 57−62.
(22) Cuppoletti, C. M.; Rothberg, L. J. Persistent Photoluminescence in Conjugated Polymers. *Synth. Met.* **2003**, *139*, 867−871.
(23) Khan, M. I.; Bazan, G. C.; Popovic, Z. D. Evidence for Electric Field-Assisted Dissociation of the Excited Singlet State into Charge Carriers in MEH-PPV. *Chem. Phys. Lett.* **1998**, *298*, 309−314.
(24) Pope, M.; Swenberg, C. E. *Electronic Processes in Organic Crystals and Polymers*; Oxford University Press: New York, 1999.
(25) Wang, P.; Collison, C. J.; Rothberg, L. J. Origins of Aggregation Quenching in Luminescent Phenylenevinylene Polymers. *J. Photochem. Photobiol., A* **2001**, *144*, 63−68.


DOI: 10.1021/acs.jpca.5b11349
*J. Phys. Chem. A* 2016, 120, 551−555